DOI: 10.3901/CJME.2015.0228.020, available online at www.springerlink.com; www.cjmenet.com; www.cjme.com.cn

Analysis of Thermoelastohydrodynamic Performance of Journal Misaligned Engine Main Bearings

BI Fengrong*, SHAO Kang, LIU Changwen, WANG Xia, and ZHANG Jian

State Key Laboratory of Engines, Tianjin University, Tianjin 300072, China

Received March 13, 2014; revised February 17, 2015; accepted February 28, 2015

Abstract: To understand the engine main bearings' working condition is important in order to improve the performance of engine. However, thermal effects and thermal effect deformations of engine main bearings are rarely considered simultaneously in most studies. A typical finite element model is selected and the effect of thermoelastohydrodynamic(TEHD) reaction on engine main bearings is investigated. The calculated method of main bearing's thermal hydrodynamic reaction and journal misalignment effect is finite difference method, and its deformation reaction is calculated by using finite element method. The oil film pressure is solved numerically with Reynolds boundary conditions when various bearing characteristics are calculated. The whole model considers a temperature-pressure-viscosity relationship for the lubricant, surface roughness effect, and also an angular misalignment between the journal and the bearing. Numerical simulations of operation of a typical I6 diesel engine main bearing is conducted and importance of several contributing factors in mixed lubrication is discussed. The performance characteristics of journal misaligned main bearings under elastohydrodynamic(EHD) and TEHD loads of an I6 diesel engine are received, and then the journal center orbit movement, minimum oil film thickness and maximum oil film pressure of main bearings are estimated over a wide range of engine operation. The model is verified through the comparison with other present models. The TEHD performance of engine main bearings with various effects under the influences of journal misalignment is revealed, this is helpful to understand EHD and TEHD effect of misaligned engine main bearings.

Keywords: main bearings, journal misaligned, oil film pressure, Reynolds equation, finite difference methods, thermoelastohydrodynamic(TEHD)

1 Introduction

Nowadays there are more requirements for internal combustion engines with high performance and reliability to improve the journal bearings performance. With the trends in automotive industry, such as higher peak cylinder pressure, lower fuel consumption, engine downsizing and lower level of emission, all these tasks have been becoming a great challenge in the development of engine main bearings' performances.

In recent years, computer simulations have gained an increasing role in more complex simulation of technical problems even for bigger calculation domains with the increase of computer power. It is utmost necessary for research on the lubricant of main bearing for internal combustion engine. Traditional static linear finite element modeling techniques are not able to capture the nonlinearities and complex interactions among components specific to internal combustion engines[1]. Several investigations have focused on the analysis of dynamically loaded journal bearing with the purpose of emphasizing its operating properties and performance characteristics[2]. VORST, et al[3], used the finite-length impedance bearing theory to model the steady-state behavior of flexible rotor-dynamic systems bearings. OSMAN, et al[4], presented a numerical study of the performance of a dynamically loaded finite journal plastic bearing lubricated with a non-Newtonian of the bearing. The Reynolds equation was solved numerically, considering three values of the flow-behavior index and a wide range of journal speeds, materials and clearance ratios. MA, et al[5], investigated the behavior of dynamically loaded journal bearings lubricated with non-Newtonian couple stress fluids. And the film pressure was solved numerically with Reynolds boundary conditions and the various bearing characteristics were calculated. MONTAZERSADGH, et al[6], studied first dynamic load analysis of the crankshaft investigated. Finite element analysis was performed to obtain the variation of stress magnitude at critical locations while a dynamic simulation was conducted on a crankshaft. TANG[7] used a finite element method based on rectangular isoparametric element for evaluating the stiffness and

* Corresponding author. E-mail: fr_bi@tju.edu.cn

Supported by National Science and Technology Support Program of China: Vibration and Noise Reduction Technology Research and Application of Bulldozers and Other Earth Moving Machinery(Grant No. 2015BAF07B04)

damping coefficients of hydrodynamic bearings which was verified by calculated the pressure distribution of a short bearings and dynamic coefficients. AGOSTINO, et al[8], identified the journal stability threshold by using an original approximate analytical approach for the non-steady fluid film force and the stiffness and damping coefficients description in the case of low loaded porous journal bearings. ZARBANE, et al[9], presented a numerical study of the behavior of fluid film subjected to a periodic squeeze action which showed the effects of the frequency and the average film thickness on the film load-carrying ant the rupture. There were some other studies[10–16] of oil film dynamic characteristics for journal bearings analysis. All above these researches are based on journal aligned hydrodynamic bearings. In the past two years, more and more researchers[17–18] are considering the thermoelastohydrodynamic(TEHD) bearing performance as thermal effects the bearing performances.

Taking into account the couple stress effects due to the lubricants, a modified Reynolds equation for dynamic loads of the film pressure is derived by utilizing the finite difference method which is capable to predict the hydrodynamic characteristics of a thin lubricant film subjected to a periodic squeezing between conforming surfaces. In this paper, a dimensionless cycle simulation model of diesel engine has been developed that can be used to estimate the thermoelastohydrodyanmic misaligned bearing performance in a 6-cylinder 4-stroke engine with firing order 1-5-3-6-2-4. The pressure data obtained from the cycle simulation of diesel engine are introduced into the tribology model, which is a hydrodynamic lubricant analysis between crankshaft and engine block. And then journal center orbit, minimum oil film thickness and maximum oil film pressure in the main bearings are derived and presented for different engine operations when considering thermoelastohydrodynamica and different working conditions listed in this paper are length to radius ratio(λ) changes, journal misalignment, and surface roughness.

2 Calculation Method

Research on the behavior of engine main bearing under static loads is not sufficient for the design optimization. It is required to study the estimation of the dynamic load of journal bearing while the engine runs at different speeds. The model in this paper is a dynamically loaded journal bearing lubricated with an incompressible couple stress fluid. As for the analysis presented in this paper, the following assumptions were adopted:

(1)Thermal conditions;

(2) Laminar flow;

(3) Newtonian lubricant with non-compression fluid;

(4) Flex bearing surfaces;

(5) Reynolds boundary condition;

2.1 Modified Reynolds equation

Fig. 1 shows a journal rotates with angular velocity ω_j. The radius of journal is R_j and the bearing housing radius is R_b. The journal rotates with a constant angular velocity is ω_j while the bearing is stationary. The radial clearance C is defined as the distance between the journal surface and the bearing housing surface when both are concentric:

$$C = R_b - R_j. \tag{1}$$

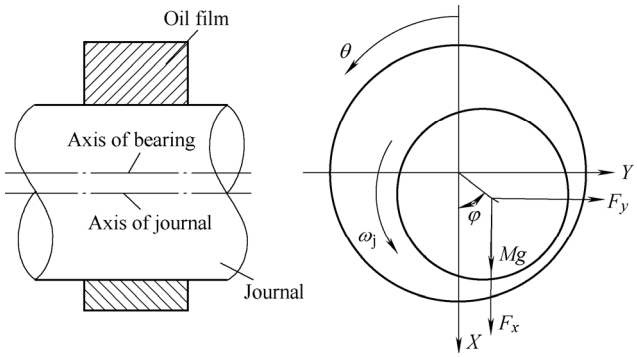

Fig. 1. Main bearing parameters

Both the journal and the bearing have the same length L in the z direction. The journal center and the bearings housing center are not always concentric due to the applied loads impacted the journal and its rotation. The distance between journal center and bearing center is e. The eccentricity ratio is ε:

$$\varepsilon = \frac{e}{C}, \quad \varepsilon \in [0, 1]. \tag{2}$$

And oil film thickness h at any angle θ for main bearing is shown as

$$h = C + e\cos(\theta - \varphi), \tag{3a}$$

where θ and φ are illustrated in Fig. 1.

In this paper, the effect of surface roughness and journal-bearing's deformation Δh was considered, then the oil film thickness changes as

$$h = C + e\cos(\theta - \varphi) + \Delta h, \tag{3b}$$

where $\Delta h = h_{rough} + h_{def}$, h_{rough} is surface roughness effect and h_{def} is journal-bearing deformation effect.

The maximum oil film thickness is h_{max}, while the minimum oil film thickness is h_{min}:

$$\begin{cases} h_{max} = C + e = C(1+\varepsilon) + \Delta h, \\ h_{min} = C - e = C(1-\varepsilon) + \Delta h. \end{cases} \tag{4}$$

The oil film pressure distribution in journal bearings is described by the Reynolds equation, which is derived from the Navier-Strokes equations for incompressible flow and

the continuity equation under simplifying assumptions[19]. For a Newtonian lubricant with non-compression fluid, the Reynolds equation under dynamic loads is written as

$$\frac{1}{R_j^2}\frac{\partial}{\partial\theta}\left(\rho h^3\frac{\partial p}{\partial\theta}\right)+\frac{\partial}{\partial z}\left(\rho h^3\frac{\partial p}{\partial z}\right)= 6\mu\left(\omega_j+\omega_b\right)\frac{\partial\rho h}{\partial\theta}+12\mu\frac{\partial\rho h}{\partial t}, \tag{5}$$

where $p(z, \theta, t)$ is the oil film pressure, ρ is the lubricant density, R_j is the crankshaft main journal radius, $h(z, \theta, t)$ is the oil film thickness, μ is the oil viscosity of film, and ω_j, ω_b is the journal angular velocity and bearing angular velocity.

Oil film temperature plays an important part in the dynamic performance of engine main bearing. The lubricant dynamic viscosity μ and density ρ are all affected with the temperature change:

$$\mu=\mu_0\exp\left(-\beta\left(T-T_0\right)\right), \tag{6a}$$

$$\rho=\rho_0\exp\left(1-\alpha_T\left(T-T_0\right)\right), \tag{6b}$$

where μ_0 is lubricant dynamic viscosity at temperature T_0, ρ_0 is lubricant density at temperature T_0, β is viscosity-temperature coefficient, α_T is coefficient of thermal expansivity.

In order to apply the finite difference method in the Reynolds equation, it is convenient to suppose the relationships of parameters and dimensionless parameters. With this purpose, the following assumptions of the dimensionless parameters are proposed:

$$\overline{h}=\frac{h}{C}=1+\varepsilon\cos\left(\theta-\varphi\right)+\frac{\Delta h}{C},\overline{z}=\frac{z}{L},\overline{p}=\frac{p\rho C^2}{6\mu\omega^* R^2},$$
$$\overline{t}=\omega t,\lambda=\frac{L}{R},q=\frac{2}{\omega^*}\frac{\mathrm{d}\varepsilon}{\mathrm{d}t},R=R_j\approx R_b, \tag{7}$$

where ω^* is the effective angular velocity, $\omega^*=\omega-2\dfrac{\mathrm{d}\varphi}{\mathrm{d}t}$, q is the dynamic parameter.

Substituting the dimensionless parameters in Eq. (7), the Reynolds equation in Eq. (5) is converted to

$$\frac{\partial}{\partial\theta}\left(\overline{h}^3\frac{\partial\overline{p}}{\partial\theta}\right)+\frac{1}{\lambda^2}\frac{\partial}{\partial\overline{z}}\left(\overline{h}^3\frac{\partial\overline{p}}{\partial\overline{z}}\right)=6\frac{\partial\overline{h}}{\partial\theta}+12\frac{\partial\overline{h}}{\partial\overline{t}}= -\varepsilon\sin\theta+q\cos\theta. \tag{8}$$

The dimensionless Reynolds equation represents the pure squeeze film behavior of journal bearing. Eq. (8) is solved by the finite difference method. In order to solve the differential Eq. (8), it is considered that atmospheric pressure prevails at the edges of the main bearing and the boundary conditions of the oil film pressure are

$$\overline{p}\,|_{\overline{z}=1}=0,\frac{\partial\overline{p}}{\partial\overline{z}}|_{\overline{z}=0}=0,\overline{p}\left(\varphi,\overline{z}\right)=\overline{p}\left(\varphi,\overline{z}+2\pi\right). \tag{9}$$

The sustentation hydrodynamic force can be calculated integrating the pressure while the hydrodynamic pressure is known. And the dimensionless loading-carrying capacity of pressure over the bearing area is calculated as

$$\overline{F}_y=\int_0^1\mathrm{d}\overline{z}\int_0^{2\pi}\overline{p}\sin\theta\mathrm{d}\theta, \tag{10a}$$

$$\overline{F}_x=\int_0^1\mathrm{d}\overline{z}\int_0^{2\pi}\overline{p}\cos\theta\mathrm{d}\theta, \tag{10b}$$

where $\overline{F}_y$, $\overline{F}_x$ is the total dimensionless force of main bearing that along axis y and axis x.

The total dimensionless oil film force $\overline{F}$ and the attitude angle, defined as the angle between the vertical axis and the line that connects the centers of the journal and the bearing housing, angle ψ is calculated by

$$\overline{F}=\sqrt{\overline{F}_y{}^2+\overline{F}_x{}^2}, \tag{11a}$$

$$\psi=\arctan\left(\frac{\overline{F}_x}{\overline{F}_y}\right). \tag{11b}$$

The force applied to the journal changes its position relative to the bearing housing, modifying the eccentricity ratio and the hydrodynamic force until equilibrium is reached. An equilibrium eccentricity ratio can then be defined as the value of ε that generates a hydrodynamic total force in the oil film with the same modulus of the external applied force[20].

2.2 Energy equations

The thermal changes behavior of oil film is determined from the energy equation when heat conduction in the circumferential and axial are all neglected.

$$\rho c_\rho\left(\frac{\partial T}{\partial t}+u\frac{\partial T}{\partial x}+v\frac{\partial T}{\partial y}+w\frac{\partial T}{\partial z}\right)= k\frac{\partial^2 T}{\partial y^2}+\mu\left[\left(\frac{\partial u}{\partial y}\right)^2+\left(\frac{\partial w}{\partial y}\right)^2\right]. \tag{12}$$

Main bearing temperature can be obtained by solving the transient heat equation which can be reduced for the simple case:

$$\rho c_\rho\frac{\partial T}{\partial t}=k\left(\frac{\partial^2 T}{\partial x^2}+\frac{\partial^2 T}{\partial z^2}\right). \tag{13}$$

2.3 Journal misalignment

Journal misalignment is one of the most important faults of journal bearings. Journal misalignment can be a particular working bearing condition, due to the deformations of the bearing system. Fig. 2 shows a journal

misalignment bearing. The main difference between misaligned bearing and aligned bearing is oil film thickness between journal and bearing. The dimensionless oil film thickness of this misaligned bearing can be calculated[21] by

$$\bar{h} = \tan\Lambda\left(z-\frac{L}{2}\right)\cos\left(\theta-\alpha-\Phi_0\right)\Big/C + 1+\varepsilon_0\cos\left(\theta-\Phi_0\right)+\delta_{\mathrm{r}}+\delta_{\mathrm{d}}, \tag{14}$$

where ε_0 is eccentricity of aligned bearing and ε' is the misaligned journal bearing. α is the angle between the journal rear center-line projection and eccentricity vector. Λ is the angle of journal misalignment, which means the included angle between journal center line and bearing center line, the bearing center line means Z axis. The included angle between journal center line and axis X and axis Y is defined as Λ_x and Λ_y. And the changes of these angles are A_x and A_y. Φ_0 is the angle between the journal vertical center-line and X axis. δ_{r} is main bearing's surface roughness. δ_{d} is main bearing's deformation.

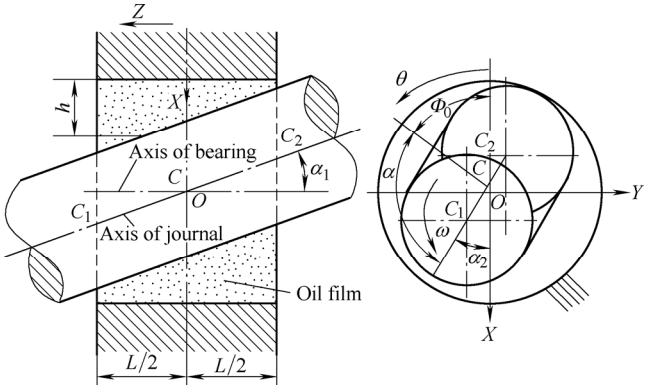

Fig. 2. Misaligned main bearing parameters

2.4 Numerical solution method

The theoretical aspects of the algorithm were already presented. The next section will explain numerical solution methods of the simulation. The centered finite difference method is used in the governing the Reynolds equation, which was used in the oil film pressure. All these programs will be executed in MATLAB.

The centered finite difference method that is used in the governing equations was integrated by iterative techniques. Derivatives in Reynolds equation were expressed by suing second order, centered finite differences[22]:

$$\begin{cases} \dfrac{\partial p}{\partial\theta}(i,j) \approx \dfrac{p(i+1,j)-p(i-1,j),}{2\Delta\theta} \\ \dfrac{\partial p}{\partial z}(i,j) \approx \dfrac{p(i,j+1)-p(i,j-1),}{2\Delta z} \\ \dfrac{\partial^2 p}{\partial\theta^2}(i,j) \approx \dfrac{p(i+1,j)-2p(i,j)+p(i-1,j),}{\Delta\theta^2} \\ \dfrac{\partial^2 p}{\partial z^2}(i,j) \approx \dfrac{p(i,j+1)-2p(i,j)+p(i,j-1)}{\Delta z^2}. \end{cases} \tag{15}$$

Based on the central difference method for derivatives, Eq. (8) changes as

$$p_{(i,j)} = \frac{A\bullet p_{(i+1,j)} + B\bullet p_{(i-1,j)} + C\bullet p_{(i,j+1)} + D\bullet p_{(i,j-1)} - E}{F}, \tag{16}$$

where

$$\begin{cases} A = \bar{h}^3_{(i+1/2,j)} \\ B = \bar{h}^3_{(i-1/2,j)} \\ C = \left(\dfrac{R}{L}\right)^2\bullet\left(\dfrac{\Delta\theta}{\Delta\bar{z}}\right)^2\bullet\bar{h}^3_{(i,j+1/2)} \\ D = \left(\dfrac{R}{L}\right)^2\bullet\left(\dfrac{\Delta\theta}{\Delta\bar{z}}\right)^2\bullet\bar{h}^3_{(i,j-1/2)} \\ E = 6\left(\bar{h}_{(i+1/2,j)}-\bar{h}_{(i-1/2,j)}\right)\bullet\Delta\theta+12\left(\dot{x}\cos\theta+\dot{y}\sin\theta\right)\bullet\Delta\theta^2 \\ F = A+B+C+D \end{cases}$$

An equally spaced computational grid is covered in this paper. The numbers of internals in the axial and in the radial direction size is 400×40 which gives a rapid rate of convergence and suitable computer working time. And a linear equation system which is in the same number of unknown pressure was determined when boundary condition was determined. The iterative procedure is terminated when the difference tolerance is

$$\delta = \frac{\sum\sum\left|p_{i,j}^{(k+1)}-p_{i,j}^{(k)}\right|}{\sum\sum\left|p_{i,j}^{(k+1)}\right|} \leqslant 10^{-5}. \tag{17}$$

Fig. 3 shows the general solution flowchart of main journal bearing that is used in this study. It gives a general overview of the algorithm and summarizes all steps.

2.5 Validation

In order to test the validity of present analysis, a 4-cylinder 4-stroke engine was firstly present, and the test data of structural parameters, etc. of crankshaft and bearing given in SUN, et al[23], were used. Figs. 4 and 5 show the comparison of the maximum film pressure of #1 connecting rod bearing and #4 main bearing in an engine cycle under dynamic loads with rotational speed 2600 r/min. In Figs. 4 and 5, the maximum oil film pressure of #1 big end bearing and #4 main bearing are calculated in good agreement with SUN, et al[23]. The difference in the maximum oil film pressure can be attributed to different gas pressures and different main parts properties.

These two comparisons validate the application of the proposed theory and model for the rest part of the presented results. It also confirms that the method used in this paper is agreeable with the fact and it can be used in other realistic engine bearings analysis. And the accuracy of the present lubrication analysis based on Reynolds equation is reliable.

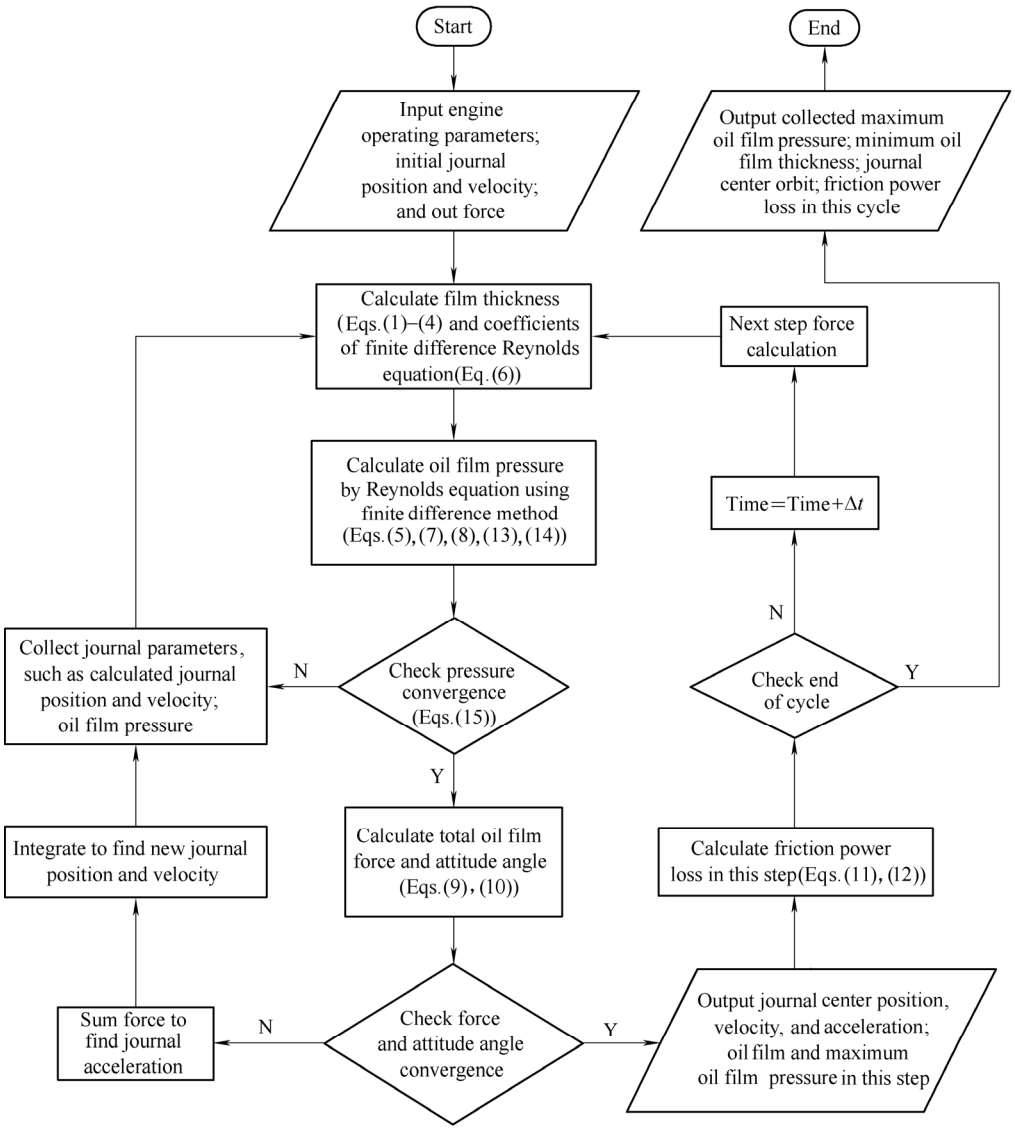

Fig. 3. General solution flowchart of engine main journal bearing

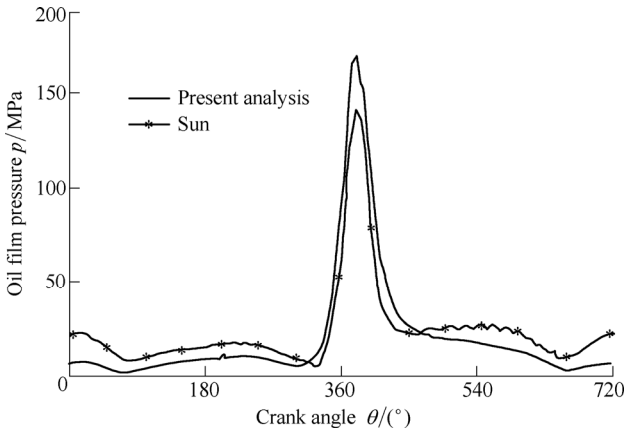

Fig. 4. Maximum oil film pressure for SUN's #1 big end bearing with rotational speed 2600 r/min

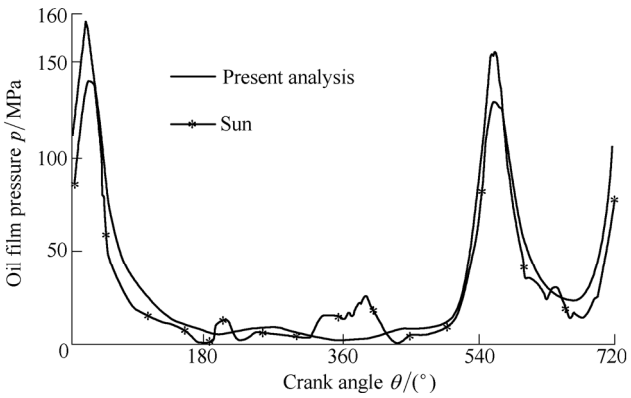

Fig. 5. Maximum oil film pressure for SUN's #4 main bearing with rotational speed 2600 r/min

3 Results and Discussions

3.1 Gas forces and main bearing load

Forces in a diesel engine may be divided into inertia forces and pressure forces. Inertia forces are divided into two objects: rotating inertia forces and reciprocating inertia forces. There are two main forces that engine block is affected in its work, one is gas force in cylinder, the other is inertia force and moment that is made by moving parts, such as piston slap force and main bearing force. Gas

forces in cylinders affects piston head, cylinder head and on side wall of the cylinder. The gas forces are transmitted to the crankshaft through the piston and connecting rod. In this study, cylinder pressure curves for 7.0 L diesel engine studied under full load at 2300 r/min over the cycle simulation corresponding to Fig. 6. As shown in Fig. 6, the highest pressure is 17.97 MPa and the fire order is 1-5-3-6-2-4.

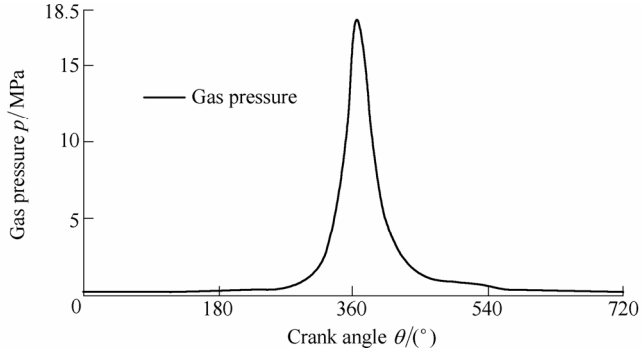

Fig. 6. Gas pressure at 2300 r/min

The effect of load on pressure in a cylinder could be estimated with the cycle simulation. The pressure in the cylinder was introduced into the lubrication model of the engine main bearings[24]. There are two different loads acting on the main bearings. One is the inertia of rotating components that applies forces to the crankshaft and this force increases with the engine speed up. The other load is source force applied to the crankshaft due to the gas combustion in the cylinder bore. Fig. 7 shows loads on the #2 main bearing over the engine cycle. There the Y and Z are the hydrodynamic forces in horizontal and vertical directions, respectively.

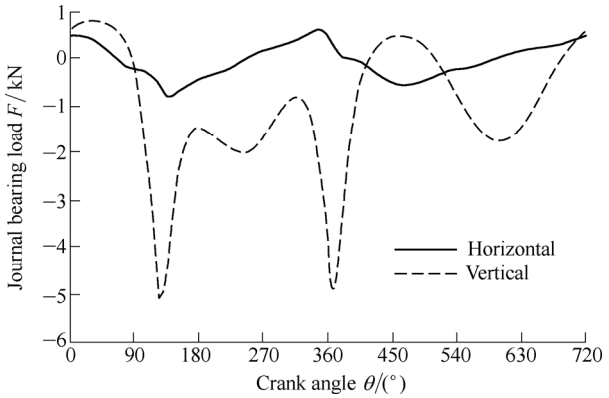

Fig. 7. Calculated main bearing loads of #2 main bearing in horizontal and vertical direction

3.2 Length to radius effect

Considering mathematical model, the governing parameters are eccentricity ratio(ε), length to radius ratio(λ). In order to accomplish this simulation, the configuration parameters of the main bearings are modeled as λ=0.75, λ=1.00, λ=1.25, and main journal bearing variables used in this paper are listed in Table 1.

Table 1. Configuration Parameters of the Crankshaft Bearings

Name	Value
Rotational speed/(r • min^{-1})	2300
Radius of main bearing/mm	42.5
Radial clearance/mm	0.03
Oil film viscosity/(MPa • s)	11
Radius of connecting rod/mm	32.5
Length of connecting rod/mm	29.5
Constant temperature of lubricant/℃	110
Constant oil supply pressure/MPa	0.5

Fig. 8 shows the comparison of journal center orbits in different λ of #2 main journal bearing. As shown, for different λ, the orbits of journal center are similar in shape. With the increase of λ, the journal center orbit gradually shrinks to the center of the journal which indicates that λ benefits to the increase of the oil film thickness in the dynamically loaded bearings. The minimum oil film thickness h_{min} and the maximum oil film pressure p_{max} in different λ are showed in Fig. 9 and Fig. 10 respectively. The results show that lubricant is affected by λ under compression and expansion stokes. Fig. 9 presents the comparison of the minimum oil film thickness of #2 main bearing by considering elasohydrodynamic effect and TEHD effect. The minimum oil film thickness increases in these three different models when considering thermo effect. And also the minimum oil film thickness increases with the increase of λ. As indicated in Fig. 10, under the dynamic loads the maximum oil film pressure is decreased while λ is enhanced. The thermo affects the maximum oil film pressure and makes it decreases. All these trends are similar with FATU's, et al[25], work.

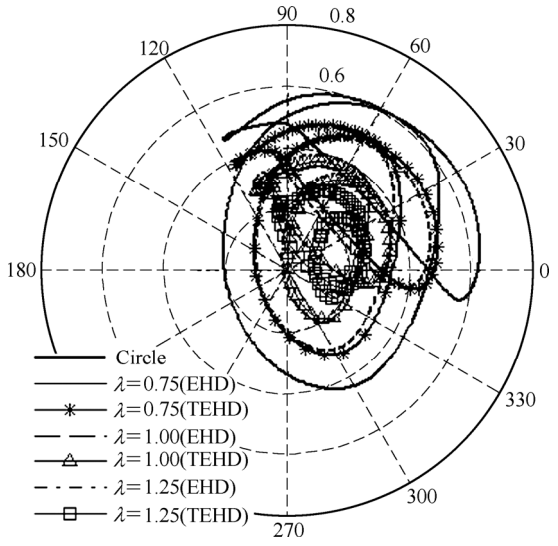

Fig. 8. Comparison of journal center orbits in different λ of #2 main journal bearing

3.3 Surface roughness effect

Bearing surfaces, even after the most careful polishing, will still be rough at a microscopic scale[26]. Based on Refs. [27–28], the RMS surface roughness of main journal

bearing is considered as 0.15 μm. And the typical surface topography digitized from the ground main journal surface is shown in Fig. 11. As shown in Fig. 11, the numerical surface roughness is random generated by using MATLAB. The number of surface nodes is 400×40, which was corresponded to the dimension of the oil film's distribution. The roughness size is included in the Δh, which was defined in Eqs. (3b) and (4).

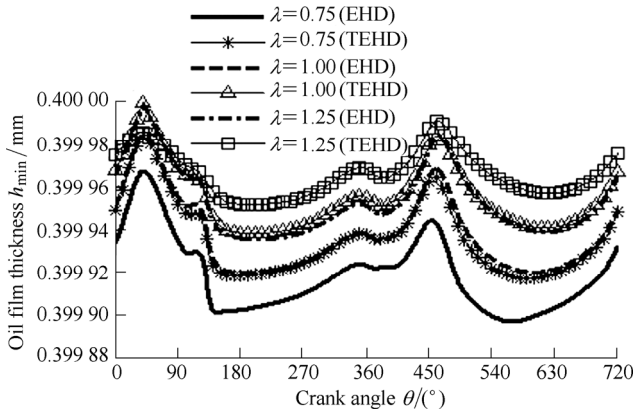

Fig. 9. Comparison of minimum oil film thickness of #2 main bearing in different λ

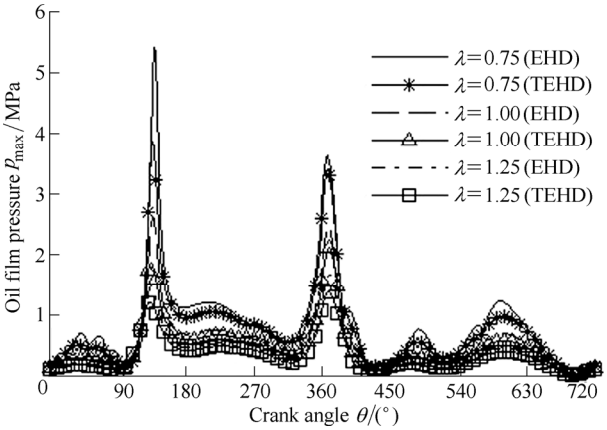

Fig. 10. Comparison of maximum oil film pressure of #2 main bearing in different λ

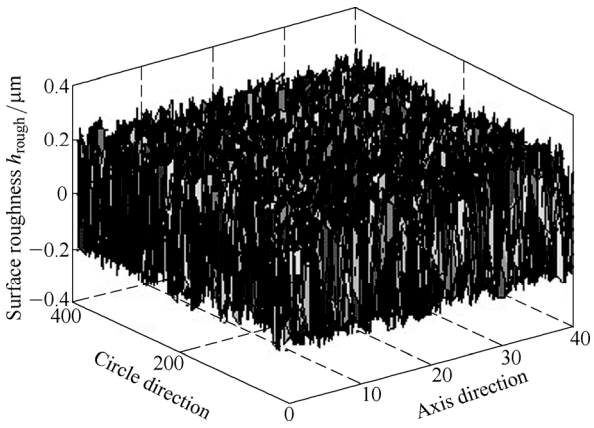

Fig. 11. Typical digitized 3D main journal surface profile used in the dynamic simulation

Fig. 12 shows the comparison of journal center orbits by considering smooth surface and rough surface of #2 main journal bearing under EHD and TEHD working conditions. As shown in this figure, the shape of journal center orbit expands with rough surface effect. And when considering the thermal effect, the shape of journal center orbit shrinks. Fig. 13 and Fig. 14 shows the comparisons of minimum oil film thickness and maximum oil film pressure respectively. When consider surface roughness effect, the minimum oil film thickness decreases and maximum oil film pressure increases in both EHD and TEHD working conditions. And also, when considering the thermal effect, the minimum oil film thickness is larger than that without thermal effect. And the maximum oil film pressure is smaller than that without thermal effect.

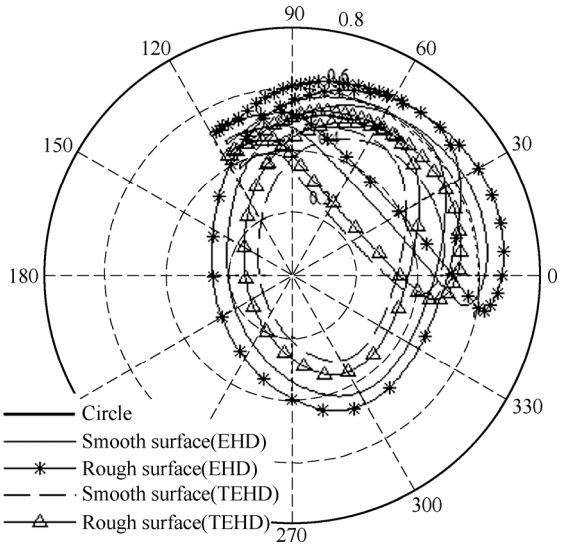

Fig. 12. Comparison of journal center orbit of #2 main bearing in different surface roughness

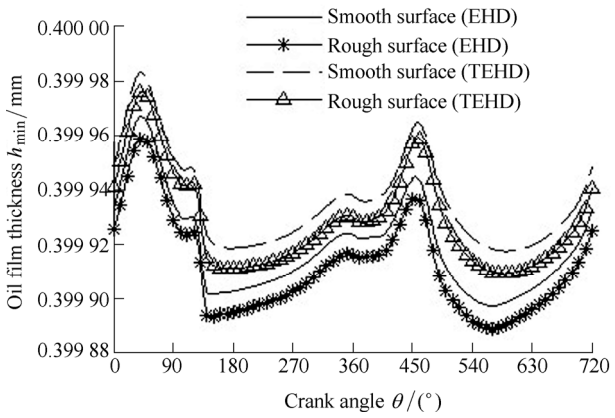

Fig. 13. Comparison of minimum oil film thickness of #2 main bearing in different surface roughness

3.4 Journal misalignment effect

Misalignment is one of the most important faults of main journal bearing. With the deformation of the journal and bearing, misalignment of main bearing is inevitable. Figs. 15–17 show the effect of journal misaligned angle with and without considering thermal effect. In these figures, Ax means the included angle changes between journal center line with the positive of x axis and Ay means the angle changes between journal center line with y axis positive.

And the original journal center line coaxial with bearing center line. A_x=0.0°, A_y=0.0° means a center line aligned bearing. Fig. 15 gives journal center orbit changes with a variety of the misaligned angle. It is shown that with the increase of misaligned angle, the shape of journal center orbit expands. When consider thermal effect, the orbit outline is smaller than the non-thermal effect journal. Fig. 16 shows the minimum oil film thickness of main bearing #2 in different misaligned angle. With the increase of misalign angle, the minimum oil film thickness increase while the minimum position change a lot. When the journal misaligned angle A_x=0.0°, A_y=0.0°, the curve of journal center orbit, minimum oil film thickness and maximum oil film pressure are all the same with Figs. 12−14, while considering surface roughness. Fig. 17 shows the maximum oil film pressure in a working cycling. The trends of maximum oil film pressure are almost in the same way. And the maximum oil film pressure increased with the increase of the misaligned angle. The lower pressure can be got when thermal effect is considered. The different between them are almost 2 MPa.

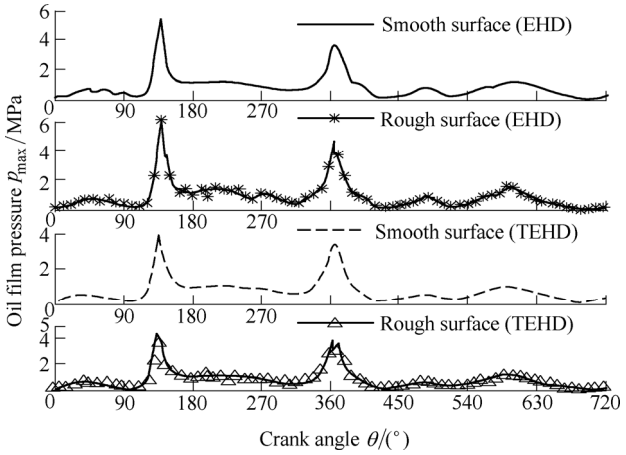

Fig. 14. Comparison of maximum oil film pressure of #2 main bearing in different surface roughness

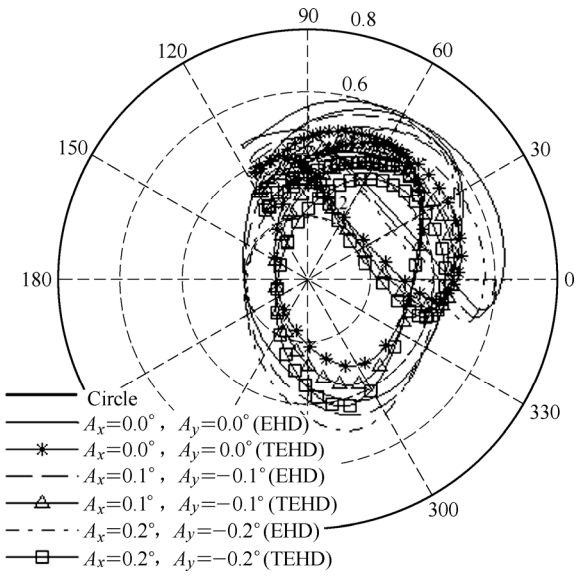

Fig. 15. Comparison of journal center orbit of #2 main bearing in different journal misaligned angle

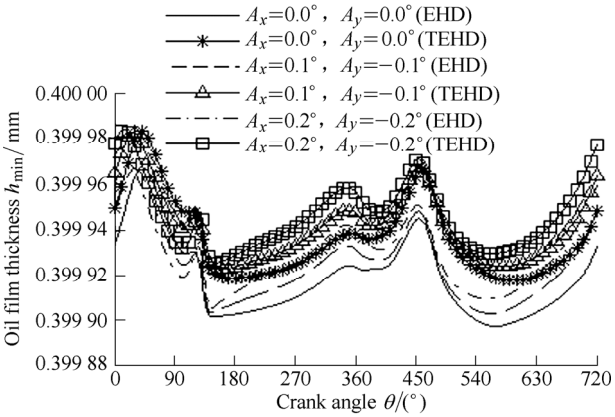

Fig. 16. Comparison of minimum oil film thickness of #2 main bearing in different journal misaligned angle

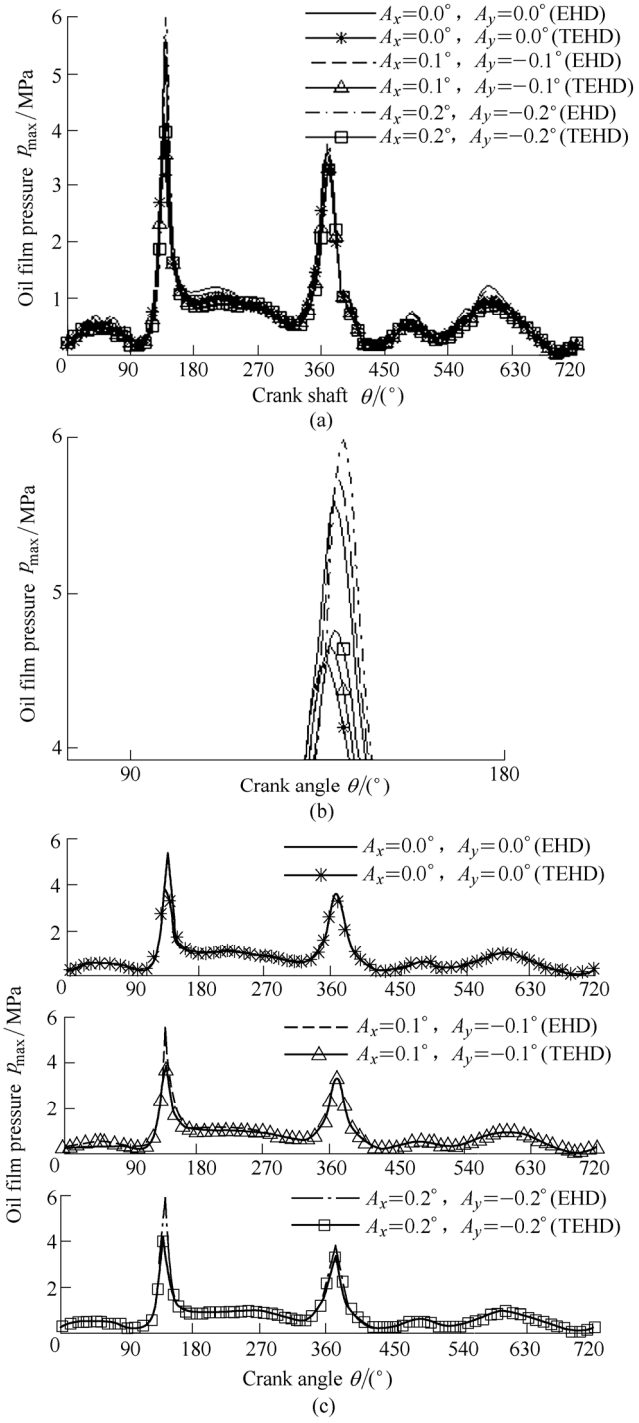

Fig. 17. Comparison of maximum oil film pressure of #2 main bearing in different journal misaligned angle

4 Conclusions

(1) For dynamically loaded of journal bearing lubricated with nonlinear fluid, the influence of λ, surface roughness and misaligned angle are significant apparently. With the increase of λ, the minimum oil film thickness increases, the maximum oil film pressure decreases. With the increase of surface roughness, the minimum oil film thickness and maximum oil film are all decreased. With the increase of misaligned angle, the minimum oil film thickness and maximum oil film are all increased.

(2) TEHD effect should be considered in bearing performance calculation because it can decrease the minimum oil film thickness and maximum oil film pressure than that calculated with elastohydrodynamic effect.

(3) Pressure in the cylinder over the engine cycle is introduced into the hydrodynamic lubrication analysis of engine main bearing. The journal center orbits that occurs a variety of phenomenon, the bearing is driven by a dynamically load. And all full hydrodynamic model of the main bearing should be considered by the realistic orbit results.

(4) Bearing performance calculated by using the finite difference method is a simple convenient, time saving, and high precision method in the calculate engine main bearings. And the model can also be used in analysis of other compressors and reciprocating engines with transient load which is supported by bearings.

References

[1] BELOIU D M. Modeling and analysis of powertrain NVH[G]. *SAE Technical Paper*, 2012-01-0888.

[2] PANDA S, MISHRA D. A multi-objective optimum design of dynamically loaded journal bearing for a prescribed π extent film[G]. *SAE Technical Paper*, 2009-01-1679.

[3] VAN DE VORST E L B, FEY R H B, DE KRAKER A, et al. Steady-state behaviour of flexible rotordynamic systems with oil journal bearings[J]. *Nonlinear Dynamics*, 1996, 11(3): 295–313.

[4] OSMAN T A, NADA G S, SAFAR Z S. Different magnetic models in the design of hydrodynamic journal bearings lubricated with non-Newtonian ferrofluid[J]. *Tribology Letters*, 2003, 14(3): 211–223.

[5] MA Y Y, WANG W H, CHENG X H. A study of dynamically loaded journal bearings lubricated with non-Newtonian couple stress fluids[J]. *Tribology Letters*, 2004, 17(1): 69–74.

[6] MONTAZERSADGH F H, FATEMI A. Dynamic load and stress analysis of a crankshaft[G]. *SAE Technical Paper*, 2007–01–0258.

[7] TANG B. Computing the main journal bearings dynamic coefficients in a six-cylinder in-line diesel engine[G]. *SAE Technical Paper*, 2007-01-1968.

[8] D'AGOSTINO V, RUGGIERO A, SENATORE A. Unsteady oil film forces in porous bearings: analysis of permeability effect on the rotor linear stability[J]. *Meccanica*, 2008, 44(2): 207–214.

[9] ZARBANE K, ZEGHLOUL T, HAJJAM M. A numerical study of lubricant film behaviour subject to periodic loading[J]. *Tribology International*, 2011, 44(12): 1659–1667.

[10] EBRAT O, MOURELAOS Z P, VLAHOPOULOS N, et al. Oil film dynamic characteristics for journal bearing elastohydrodynamic analysis based on a finite difference formulation[G]. *SAE Technical Paper*, 2003–01–1669.

[11] CHENG M, MENG G, JING J P. Non-linear dynamics of a rotor-bearing-seal system[J]. *Archive of Applied Mechanics*, 2006, 76(3): 215–227.

[12] SHEEN Y T, LIU Y H. A quantified index for bearing vibration analysis based on the resonance modes of mechanical system[J]. *Journal of Intelligent Manufacturing*, 2009, 23(2): 189–203.

[13] EI-MARHOMY A A. Dynamics and stability of elastic shaft-bearing systems with nonlinear bearing parameters[J]. *Heat and Mass Transfer*, 1999, 35(4): 334–344.

[14] KURKA P R G, IZUKA J H, PAULINO K L G. Dynamic loads of reciprocating compressors with flexible bearings[J]. *Mechanism and Machine Theory*, 2012, 52: 130–143.

[15] CRUZ R F D, GALLI L A F. Comparison of hydrodynamic and elastohydrodynamic simulation applied to journal bearings[G]. *SAE Technical Paper*, 2010-36-0360.

[16] SUN J, ZHAO X Y, WANG H. Lubrication Analysis of crankshaft bearing considering crankshaft deformation[G]. *SAE Technical Paper*, 2011-01-0613.

[17] ZHANG Z S, DAI X D, XIE Y B. Thermoelastohydrodynamic behavior of misaligned plain journal bearings[J]. *Proceedings of the Institution of Mechanical Engineers, Part C: Institution of Mechanical Engineers Science*, 2013, 227(11): 2582–2599.

[18] ZHAO X Y, SUN J, WANG C M, et al. Study on thermoelastohydrodynamic performance of bearing with surface roughness considering shaft deformation under load in shaft-bearing system[J]. *Industrial Lubrication and Tribology*, 2013, 65(2): 119–128.

[19] PINKUS O, STTERNLICHT B. *Theory of hydrodynamic lubrication*[M]. McGraw Hill Inc., 1961.

[20] SALLES B, BITTENCOURT M L, CRUZ R, et al. Radial surface bearing optimization for internal combustion engines[G]. *SAE Technical Paper*, 2009-36–0191.

[21] SUN J, GUI C L. Hydrodynamic lubrication analysis of journal bearing considering misalignment caused by shaft deformation[J]. *Tribology International*, 2004, 37(10): 841–848.

[22] DURAK E, KURBANOĞLU C, BIYIKLIOĞLU A, et al. Measurement of friction force and effects of oil fortifier in engine journal bearings under dynamic loading conditions[J]. *Tribology International*, 2003, 36(8): 599–607.

[23] SUN J, GUI C L. Effect of lubrication status of bearing on crankshaft strength[J]. *Journal of Tribology-Transactions of the ASME*, 2007, 129(4): 887–894.

[24] OZASA T, NIIZEKI M, SAKURAI S, et al. Lubrication analysis of a con-rod bearing using a cycle simulation of gasoline engines with a/f variation[G]. *SAE Technical Paper*, 2011-01-2118.

[25] FATU A, HAJJAM M, BONNEAU D. A new model of thermoelastohydrodynamic lubrication in dynamically loaded journal bearings[J]. *Journal of Tribology-Transactions of the ASME*, 2006, 128(1): 85–95.

[26] JAGADEESHA K M, NAGARAJU T, SHARMA S C, et al. 3D surface roughness effects on transient non-newtonian response of dynamically loaded journal bearings[J]. *Tribology Transactions*, 2012, 55(1): 32–42.

[27] LEOPOLD J. Surface quality control using biocomputational algorithms[J]. *Journal of Intelligent Manufacturing*, 1998, 9: 377–382.

[28] DENKENA B, HENNING H. Multicriteria dimensioning of hard-finishing operations regarding cross-process interdependencies[J]. *Journal of Intelligent Manufacturing*, 2010, 23(6): 2333–2342.

Biographical notes

BI Fengrong, born in 1965, is currently a professor at *Tianjin University, China*. He received his PhD degree from *Tianjin University, China,* in 2003. His research interests include engine noise and vibration control, automobile dynamics, etc.

Tel: +86-13802167153; E-mail: fr_bi@tju.edu.cn

SHAO Kang, born in 1981, is currently a PhD candidate at *State Key Laboratory of Engines, Tianjin University, China*. He received his master degree from *Tianjin University, China*, in 2009. His research interests include engine crankshaft dynamic.
Tel: +86-15822457519; E-mail: kangshao1981@tju.edu.cn

LIU Changwen, born in 1963, is currently a professor at *Tianjin University, China*. His research interest is engine's electronic control technology.
E-mail: liuchangwen@tju.edu.cn

WANG Xia, born in 1984, is currently a PhD candidate at *State Key Laboratory of Engines, Tianjin University, China*. She is currently studying the digital signal processing of engine's noise and vibration.
E-mail: wangxia@tju.edu.cn

ZHANG Jian, born in 1983, is currently a PhD candidate at *State Key Laboratory of Engines, Tianjin University, China*. He is currently studying the engine vibration signal processing.
E-mail: neil1101@tju.edu.cn